Collision-Free Trajectory Planning for Manipulator Using Virtual Force based Approach

P. Chotiprayanakul, D. K. Liu, D. Wang, G. Dissanayake
ARC Centre of Excellence for Autonomous Systems
Faculty of Engineering, University of Technology, Sydney
Broadway, NSW 2007, Australia
{pchotipr, dkliu, Da-Long.Wang, gdissa}@eng.uts.edu.au

Abstract - **This paper presents a virtual force based approach for real-time collision-free trajectory planning for manipulators. This approach defines a virtual attractive force to drive an end-effecter of a manipulator along a preplanned path and uses virtual repulsive force calculated based on 3-dimensional force field method (3D-F^2) to protect the whole robot arm. When all these external virtual forces are applied to a manipulator's dynamic model, the wire model of the manipulator, which is modeled by using virtual joints with stiffness and damping, will move to the steady state of the manipulator's dynamics model at the target point. At every time step, this approach outputs a pose or joint angles of the robot arm to the robotic manipulator controller to control the real robot arm through. Simulation results show that this approach can manage to find the trajectory of a robot arm in a very narrow environment without colliding into obstacles.**

Keywords – **3D-F^2, force field, collision avoidance, motion planning**

I. INTRODUCTION

In manipulator trajectory planning, given a target point, the poses of a robot arm along the trajectory is generated by applying inverse kinematics approach or optimization approach. Collision-free trajectory planning is one of the big issues in motion planning. For a whole robot arm, the trajectory planning has to take the geometry of environments and dimension of the manipulator into account. For increasing the efficiency of planning and collision avoidance, researchers have been trying to cover robot manipulator links and obstacles with known shapes such as ellipsoid, spheres, etc. Efficiency of planning has significant effect on the performance of real time control of the manipulator especially in unknown/dynamic environments.

Path/motion planning and collision avoidance have been extensively investigated. Biegelbauer et al. generalized the painting path planning process, which is capable of generating collision-free trajectory for the end-effecter [1]. R Saravanan,, S. Ramabalan, et al. combined objective functions and constraints to find optimal collision free trajectory for an end-effecter [2]. Both papers did not present the collision avoidance for the whole body of a robot arm. For collision avoidance of the whole manipulator, Lozano-Perez presented approaches to distance measuring between polyhedrons which are used for path planning in discrete C-space [3][4]. The disadvantage of this method is that it is time consuming to construct configuration space for a manipulator with higher DOFs and difficult for real time applications. Potential field method and its varieties perhaps are the most popular approaches for online collision avoidance [5]. Juang applied polyhedrons to represent a manipulator and potential field method to control of a manipulator [6][7]. Greenspan and Burtnyk modeled a robot and obstacles with sets of spheres, measured the distances with a weighted voxel map and demonstrated successful collision avoidance and on-line path planning [8][9]. Lin and Chuang used potential fields in 3-D workspace to generate a collision free path by locally adjusting the robot configuration for minimum potential [10]. Brock and Khatib presented elastic strip framework generating an obstacle bended free space tunnel for a robot to move from point to point [11]. Xie et al. used spheres covering a robot arm and converted the repulsive forces to joint torques to disturb the conventional manipulator's dynamic system and the collision-free trajectory will be worked out [12]. Wang et al. [13] presented a variable speed force field (VSF^2) method in 2D for multi-mobile robot collaboration and collision avoidance. They defined a relationship between speed and repulsive force to reduce the oscillation in robot speed and orientation.

When a manipulator operates in obstructing environments, collision avoidance becomes a very important and difficult issue. In this paper, a collision-free trajectory is generated by a virtual force based approach. Initially, a virtual attractive force, which is defined by a distance vector between the robot arm's end-effecter position and the target position, "pulls" the end-effecter of the robot to the target point. Meanwhile, virtual repulsive forces from obstacles nearby, which are calculated from a 3D-F^2 method, will alter the trajectory to prevent the whole robot body from collisions. The concept of the virtual force based collision-free trajectory planning provides an efficient way to control manipulators by just relating the virtual force based controller to a manipulator's position controller. In section II, we describe a robot model, the definition of attractive force and a 3D-F^2 [14]. A new dynamic control model with collision avoidance algorithm is given in Section III. Simulation results are presented in Section IV followed by conclusions and future work in Section V.

II. METHODOLOGY

In this section, we will start from establishing a robot model for Denso 6556[15]. The definition of attractive force and 3D-F^2 are then introduced.

A. *Robot Model*

A robot arm is represented with a wire model (Fig.1). Every joint of the robot arm is represented by a virtual joint with stiffness and damping. Every joint in this dummy model can be rotated or twisted by external forces. When external forces disappear, a joint will spring back to its initial position as a result of virtual interior spring force.

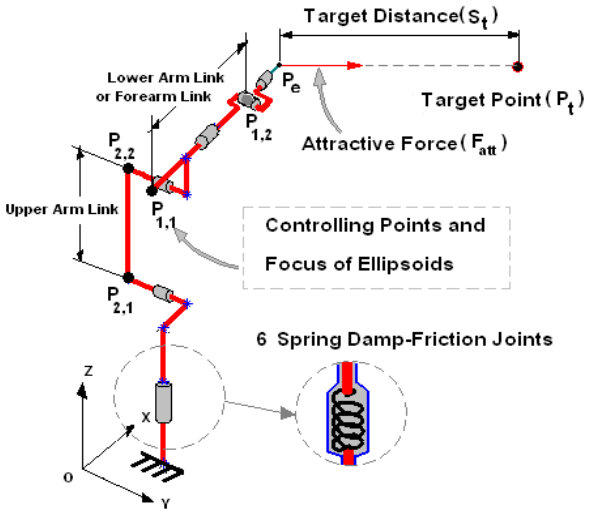

Fig. 1. The robot model and attractive force

B. *Attractive Force*

Given a target point, a virtual attractive force that "pulls" the end-effecter to the target point will be generated. This attractive force can be defined by the distance between the current position of the manipulator's end-effecter and the target position. The amplitude of the attractive force is limited by a force factor (K_{att}) and given by (2) to (4), where K_{zero} is a small non-zero positive constant and K_s is a constant, which will determine how the attractive force varies with the distance between the end-effecter and the target point. The amplitude of the attractive force increases with the distance and its direction is set to be from the current position of end-effecter to the target.

$$S_t = \left|\vec{\mathbf{P}}_\mathbf{t} - \vec{\mathbf{P}}_\mathbf{e}\right| \tag{1}$$

$$\left|\vec{\mathbf{F}}_{\mathbf{att}}\right| = \frac{K_{att}}{1+\left(\frac{e^{-K_s S_t}}{K_{zero}}\right)} \tag{2}$$

$$\vec{\mathbf{F}}_{\mathbf{att}\,unit} = \frac{\vec{\mathbf{P}}_\mathbf{t} - \vec{\mathbf{P}}_\mathbf{e}}{S_t} \tag{3}$$

$$\vec{\mathbf{F}}_{\mathbf{att}} = \vec{\mathbf{F}}_{\mathbf{att}\,unit} * \left|\vec{\mathbf{F}}_{\mathbf{att}}\right| \tag{4}$$

C. *Definition of 3D-F²*

This section introduces the 3D-F² defined in [14]. The transformations from the robot's coordinate system to the global system are given by transfer function ($^i\mathbf{T}_j$) and rotation-translation metrics ($^i\mathbf{A}_j$). $\mathbf{P}_{i(u,v,w)}$ and $\mathbf{P}_{i(x,y,z)}$ are points on the robot's coordinate system and the global system, respectively.

$$^0\mathbf{T}_1 = {}^0\mathbf{A}_1 \tag{5}$$

$$^0\mathbf{T}_2 = {}^0\mathbf{A}_1\,{}^1\mathbf{A}_2 \tag{6}$$

$$^0\mathbf{T}_6 = {}^0\mathbf{A}_1\,{}^1\mathbf{A}_2\,{}^2\mathbf{A}_3\,{}^3\mathbf{A}_4\,{}^4\mathbf{A}_5\,{}^5\mathbf{A}_6 \tag{7}$$

$$\mathbf{P}_{1(x,y,z)} = {}^0\mathbf{T}_{n^{th}}\mathbf{P}_{1(u,v,w)} \tag{8}$$

$$\mathbf{P}_{2(x,y,z)} = {}^0\mathbf{T}_{n^{th}}\mathbf{P}_{2(u,v,w)} \tag{9}$$

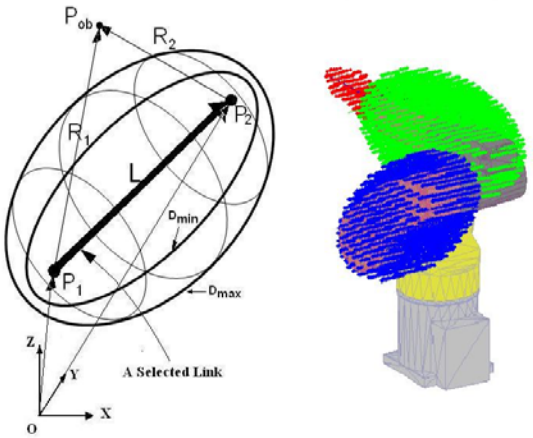

Fig. 2. (a) Parameters of D_{min} and D_{max} ellipsoid and (b) a robot arm covered by D_{min}.

To determine the ellipsoid covering a manipulator link, two points on a link are selected as the focus of the resulted ellipsoid (P_1 and P_2 in Fig. 2). To ensure that this ellipsoid will cover the whole body of the link, the length of major axis is set to be equal to L*K_p, where L is the distance between foci and K_p is a constant larger than 1. For any point in 3D space (P_{ob} in Fig. 2), if the sum of distances between this point to foci (R_1 and R_2) is equal to the length of major axis, that is, L*K_p, this point is on the ellipsoid D_{min}. If R_1+R_2 is smaller than L*K_p, this point is inside D_{min}. On the contrary, when R_1+R_2 is larger than L*K_p, the point is outside D_{min} (see Fig. 2). Thus, if *Cx* is a ratio between length of $\mathbf{R}_1$+$\mathbf{R}_2$ and length of **L**, the *Kp* will indicate $\mathbf{P}_{ob}$ is inside or outside the D_{min}. To take the linear speed of end-effecter into account, we introduce a new factor, E_r, which is a ratio of end-effecter's instant linear speed (V_i) and maximum linear speed (V_{max}) of the end-effecter of the manipulator, so E_r is between 0 to1. The length of major axis of D_{max} is equal to L*(K_p+E_r). We define:

$$Er = \frac{V_i}{V_{\max}} \tag{10}$$

$$Cx = \frac{\left|\vec{\mathbf{R}}_1\right| + \left|\vec{\mathbf{R}}_2\right|}{\left|\vec{\mathbf{L}}\right|} \tag{11}$$

Thus, the amplitude of repulsive force is given by

$$\left|\vec{\mathbf{F}}_{rep}\right| = Kf - \left(\frac{Kf}{1+e^{\left(-\frac{10\,(Cx - Kp - 0.5\,Er)}{Er}\right)}}\right) \tag{12}$$

Kf is maximum repulsive force. The repulsive force direction is defined to be the unit vector that points from $\mathbf{P}_{ob}$ to the link perpendicularly. Fig.3 shows how the amplitude of a repulsive force varies with the distance ratio: *Cx* when *Kf* = 10, *Kp* = 1.05.

$$\vec{\mathbf{F}}_{rep\_unit} = \frac{\left(\mathbf{R}_1 - dot\left(\mathbf{R}_1, \frac{\mathbf{L}}{\|\mathbf{L}\|}\right) * \frac{\mathbf{L}}{\|\mathbf{L}\|}\right)}{\left\|\mathbf{R}_1 - dot\left(\mathbf{R}_1, \frac{\mathbf{L}}{\|\mathbf{L}\|}\right) * \frac{\mathbf{L}}{\|\mathbf{L}\|}\right\|} \tag{13}$$

$$\vec{\mathbf{F}}_{rep} = \vec{\mathbf{F}}_{rep_{unit}} * \left|\vec{\mathbf{F}}_{rep}\right| \tag{14}$$

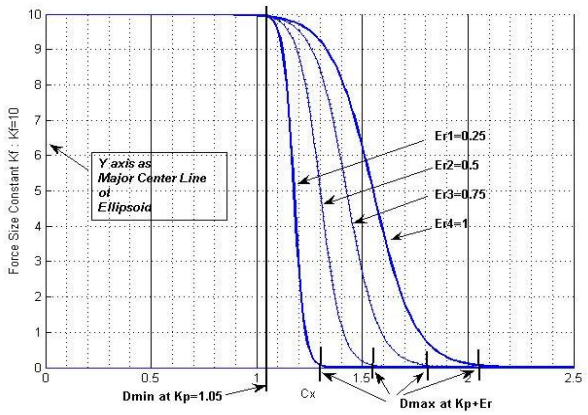

Fig. 3. A graph of the amplitude of force field with *Kf*=10, *Kp*=1.05 and *Er*.

Since *Er* is the ratio of the end-effecter's speed and its maximum linear speed, the scope of virtual force field will vary with the speed. The faster a manipulator's end-effecter moves, the more area its virtual force field will cover.

III. DYNAMICS AND COLLISION AVOIDANCE

This section introduces how to use the 3D-F^2 method for path/motion planning and real time collision avoidance. With the dummy model in Section II, the dynamic model is given by (15). The manipulator is driven by joints torques, thus all forces will be converted to the torques by Jacobian matrices in (21). The dynamic model consists of link inertias (**I**), joint damp-friction constants (**β**) and joint spring constants ($\mathbf{k}_{sp}$).

$$\boldsymbol{\tau} = \mathbf{I}\ddot{\boldsymbol{\theta}} + \boldsymbol{\beta}\dot{\boldsymbol{\theta}} + \mathbf{k}_{sp}\boldsymbol{\theta} \tag{15}$$

$${}^5\mathbf{F}_{6_{(x,y,z)}} = \mathbf{F}_{att_{(u,v,w)}} \tag{16}$$

$${}^i\mathbf{F}_{i+1_{(u,v,w)}} = \left[{}^i\mathbf{T}_{i+1}\right]^T \left({}^i\mathbf{F}_{i+1_{(x,y,z)}} + \mathbf{F}_{i+1rep_{(x,y,z)}}\right) \tag{17}$$

$$\tau_{i+1} = \mathbf{L}_{i+1_{(u,v,w)}} \times {}^i\mathbf{F}_{i+1_{(u,v,w)}} \tag{18}$$

$$\tau_{i+1} = \mathbf{L}_{i+1_{(u,v,w)}} \times \left[{}^i\mathbf{T}_{i+1}\right]^T \left({}^i\mathbf{F}_{i+1_{(x,y,z)}} + \mathbf{F}_{i+1rep_{(x,y,z)}}\right) \tag{19}$$

$$\tau_{i+1} = {}^i\mathbf{J}^T{}_{i+1}\left({}^i\mathbf{F}_{i+1_{(x,y,z)}} + \mathbf{F}_{i+1rep_{(x,y,z)}}\right) \tag{20}$$

$$\mathbf{J}^T\mathbf{F} = \mathbf{I}\ddot{\boldsymbol{\theta}} + \boldsymbol{\beta}\dot{\boldsymbol{\theta}} + \mathbf{k}_{sp}\boldsymbol{\theta} \tag{21}$$

In every control cycle, the dynamic equation (15) will give a set of joint's angles (**θ**). Then this set will be converted to current position of end-effecter (P_e) by forward transfer function ${}^0\mathbf{T}_6$ in (23). The output of (23) is sent to the robot controller. Control block diagram in Fig.4 shows the control diagram of this approach.

$$\boldsymbol{\theta} = \left[\theta_1 \;\; \theta_2 \;\; \theta_3 \;\; \theta_4 \;\; \theta_5 \;\; \theta_6\right] \tag{22}$$

$$\vec{\mathbf{P}}_e = {}^0\mathbf{T}_6[0 \quad 0 \quad 0 \quad 1]^T \tag{23}$$

In addition, when the robot is close to an obstacle and the D_{min} ellipsoid hits into the obstacle, the repulsive force will reduce the action of the attractive force acting on that link. This will prevent a robot from going further into and collision from the obstacle..

$$\vec{\mathbf{F}}'_{rep} = \begin{cases} \vec{\mathbf{F}}_{rep};\; Cx < Kp + Er \\ \vec{\mathbf{F}}_{rep} - \vec{\mathbf{F}}_{att};\; Cx \le Kp \end{cases} \tag{24}$$

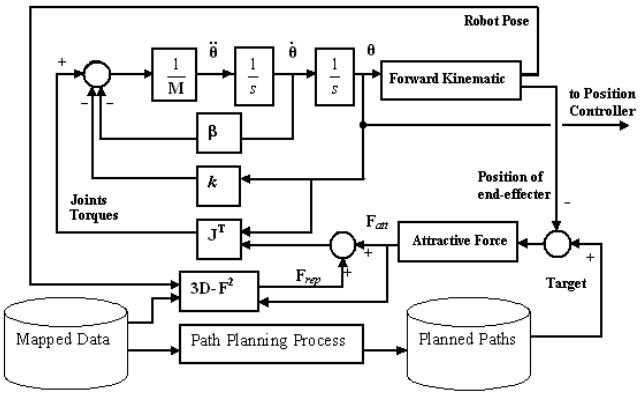

Fig. 4. The control diagram.

IV. SIMULATIONS

In the following simulations, a manipulator, Denso 6556 [15], is placed on a workbench with a partition plate close to it. The simulation program runs on MATLAB 7.1 in a Pentium 4 computer with a 2.8GHz CPU and 1GB RAM. The values of parameters in the simulations are set to be dt = 0.1 sec, *Kf* = [100 100 100], *Kp* = [1.05 1.15 1.15], **I** = [200 200 200 100 100 1], ksp = [.5 .5 .5 .001 .001 .001], K_s = 10, K_{zero} = 0.001 and K_{att} = 200. The distance between the manipulator base and the plate is 460 mm.

A. Task 1

The robot arm approaches a target behind the upper hole on the partition plate. Fig. 5 shows snapshots of the simulation with D_{min}, D_{max} and the paths. The computation time is 16 seconds in 164 iterations and total traveling distance is 1525 mm, which shows that the approach presented in this paper is suitable for real-time applications.

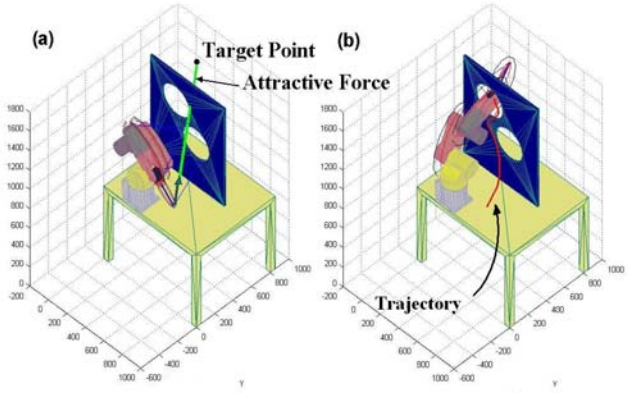

Fig. 5. Task 1: Approaching a target through a hole

B. *Task 2*

The robot arm approaches the targets behind the lower hole and the upper hole on the partition plate (point 2 and 3 in Fig.6) with the help of pre-planned intermediate goal (point 3). Fig. 6 shows simulation snapshots of the robot arm and its trajectory. Fig. 7 shows joints' angles in this simulation. The computation time is 43 seconds in 455 iterations and total traveling distance is 2220 mm.

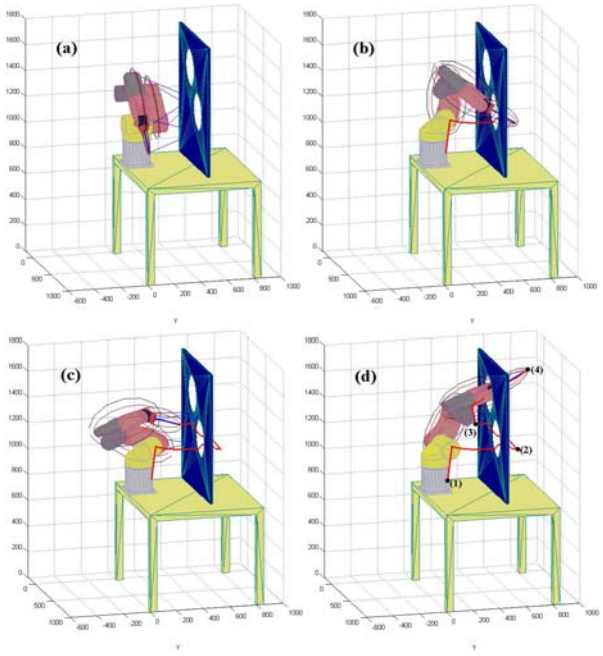

Fig. 6. Task 2: approaching multiple targets.

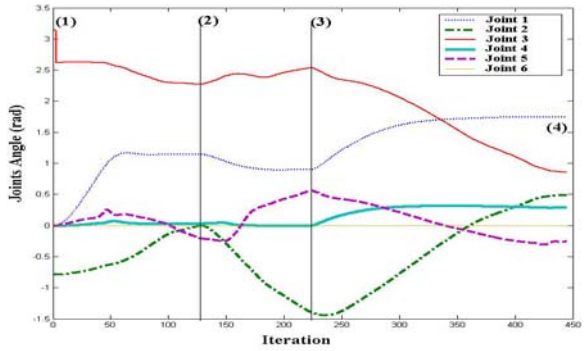

Fig. 7. The joint angles in the task 2

C. *Simulation Discussion*

The simulation results show that the virtual force based motion-planning method is able to drive the robot arm in a narrow environment without collisions. The computation speed is approximately 0.1 sec per iteration, which means this virtual force based approach is fast enough to be implemented in the real-time collision-free trajectory planning for manipulators. Simulations also show that the joints angle changes and the trajectory of the end-effecter are smooth and no sudden changes were observed. The virtual force based approach is a local method and will suffer from the existence of local minima problem. In task 2, the manipulator still needs a pre-planned intermediate goal to fulfill its task. This will be addressed in future work.

V. CONCLUSION AND FUTURE WORK

This paper presents a novel real-time collision-free trajectory planning method using the virtual force based approach. By introducing the attractive force and the 3D-F^2 method together, the virtual force based collision-free trajectory planning approach presented in the paper can be used in real applications. It is a generic approach for any type of manipulators and easy to be extended to manipulators with any DOFs. Future work will also include extending this approach to more complex cases. Multiple manipulators working in a clustered environment with some moving obstacles will be considered.

ACKNOWLEDGEMENT

This work is supported in part by the arc center of excellence for autonomous system, funded by Australian Research Council (ARC) and the New South Wales State Government, Australia.

Mr. Pholchai Chotiprayanakul is supported by Thai Government Scholarship for requirement of Industrial Engineering Department of King Mongkut's Institute of Technology Ladkrabang.

REFERENCES

[1]. G.Biegelbauer, A.Pichler, M.Vincze, C.Nielsen, H.J.Andersen, and K.Haeusler, "Automatic Generation of Robot Painting Motions for Unknown Parts", *IEEE Robotics & Automation Magazine*, 1070-9932, pp.24-34, 2005.

[2]. R.Saravanan, S.Ramabalan, et al., "Evolutionary collision-free optimal trajectory planning for intelligent robots.", International Journal on Advance Manufacturing Technology, Springer-Verlag London Limited, 2007.

[3]. T.Lozano-Perez, "Spatial Planning: A Configuration Space Approach", *IEEE Transactions on Computers*, vol. C-32, no.2, pp.108-119, 1983.

[4]. T.Lozano-Perez, "A Simple Motion-Planning Algorithm for General Robot Manipulators", *IEEE Journal of Robotics and Automation*, vol.3, pp. 224-238, 1987.

[5]. O. Khatib, "Real-Time Obstacle Avoidance for Manipulators and Mobile Robots", *IEEE International Conference on Robotics and Automation*, pp.500-505, 1985.

[6]. J.-G. Juang, "Collision Avoidance using Potential Fields", *International Journal of Industrial Robot*, MCB University Press, vol. 25, pp. 408-415, 1998.

[7]. J.-G. Juang, "Application of Repulsive Force and Genetic Algorithm to Multi-manipulator Collision Avoidance", *Proceeding of 5th Asian Conference*, vol. 2, pp.971-976, 2004.

[8]. M.Greenspan and N.Burtnyk, "Obstacle Count Independent Real-Time Collision Avoidance", *IEEE International Conference on Robotics and Automation*, Minnesota, pp.1073-1080, 1996.

[9]. M.Greenspan and N.Burtnyk, "Real Time Collision Detection", US Patent, Patent Number 5,347,459, 1994.

[10]. C.-C. Lin and J.Chuang, "Potential-Based Path Planning for Robot Manipulators in 3-D Workspace", *International Conference on Robotics Automation*, Taipei, Taiwan, pp.3353-3358, 2003.

[11]. O. Brock and O. Khatib, "Real-Time Obstacle Avoidance and Motion Coordination in a Multi-Robot Workcell", *IEEE International Symposium on Assembly and Task Planning*, Porto, Portugal, pp. 274-279, 1999.

[12]. H.P.Xie, R.V.Patel, S.Kalaycioglu and H.Asmer, "Real-Time Collision Avoidance for Redundant Manipulator in an Unstructured Environment", *IEEE International Conference on Intelligent Robots and Systems*, Victoria, B.C, Canada, 1998.

[13]. D. Wang, D.Liu and G.Dissanayake, "A Variable Speed Force Field Method for Multi-robot Collaboration", *Intentional Conference on Intelligent Robots and Systems*, Beijing, China, 2006.

[14]. P. Chotiprayanakul, et al., "A 3-Dimensional Force Field Method for Robot Collision Avoidance in Bridge Maintenance", Submitted to ISARC07.

[15]. http://www.denso-wave.com/en/robot/